Title:
Theoretical Investigation of the Curvature Monotonicity Regions of 2D Polynomial Bézier Curves based on the Sufficient Condition

Authors:
Norimasa Yoshida, yoshida.norimasa@nihon-u.ac.jp, Nihon Univeristy
Takafumi Saito, txsaito@cc.tuat.ac.jp, Tokyo University of Agriculture and Technology

Keywords:
Theoretical curvature monotonicity region, Bézier curves, implicit algebraic curves, GPU

DOI: 10.14733/cadconfP.2024.1-5

Introduction:
Freeform curves, such as Bézier curves and B-spline curves, possess numerous desirable properties and are widely used in various applications. In [11], Yoshida et al. introduced a real-time method for visualizing the curvature monotonicity regions of polynomial curves. Using the method, users can know the region of a control point for achieving monotonically varying curvature. In our current study, we theoretically investigate the curvature monotonicity regions of 2D polynomial Bézier curves, relying on the established sufficient condition. Leveraging GPU technology, we propose a real-time approach for visualizing the sufficient regions, including the implicit algebraic curves that constitute the sufficient region. The theoretical investigation allows us to provide a partial explanation for the curvature monotonicity regions.

Related work:
Numerous works have addressed the generation of freeform curves with monotonically varying curvature. The theoretical foundation for curvature monotonicity regions has been established for quadratic Bézier curves [7] and quadratic rational Bézier curves [2], elucidating both the necessary and sufficient conditions. However, for cubic or higher-degree curves, several methods have been proposed to identify the sufficient conditions. These methods include Pythagorean hodograph quintic spirals [10], Mineur's typical curves [3], 2D class A Bézier curves [1, 4] and 3D class A Bézier curves [8, 9].

Real-time visualization methods of the curvature monotonicity regions are introduced for 2D polynomial curves in [11] and for 2D rational Bézier curves in [5]. In this paper, we investigate the curvature monotonicity region of polynomial curves based on the sufficient condition.

Curvature Monotonicity Evaluation Functions:
A polynomial Bézier curve $\mathbf{P}(t)$ of degree n with $n+1$ control points $\mathbf{P}_j = [x_i \ y_i]^{\mathrm{T}} (0 \leq j \leq n)$ is defined by

$$\mathbf{P}(t) = \sum_{j=0}^{n} B_j^n(t)\mathbf{P}_j \quad (t \in [0,1]), \tag{2.1}$$

Here, $B_j^n(t)$ is a Bernstein polynomial.

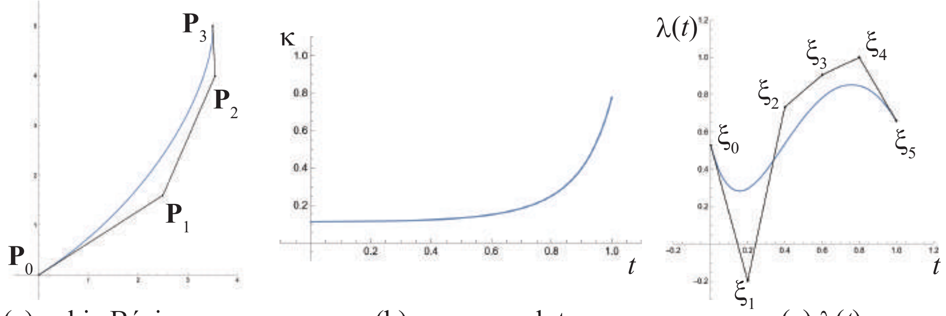

(a) cubic Bézier curve (b) curvaure plot (c) $\lambda(t)$

Fig. 1: Cubic Bézier curve, curvature plot and $\lambda(t)$.

Curvature monotonicity can be verified by checking whether $\frac{d\kappa}{ds}$ does not change its sign within $t \in [0, 1]$.

$$\frac{d\kappa}{ds} = \frac{(\dot{\mathbf{P}} \wedge \dddot{\mathbf{P}})(\dot{\mathbf{P}} \cdot \dot{\mathbf{P}}) - 3(\dot{\mathbf{P}} \wedge \ddot{\mathbf{P}})(\dot{\mathbf{P}} \cdot \ddot{\mathbf{P}})}{|\dot{\mathbf{P}}|^6}, \tag{2.2}$$

where $\dot{\mathbf{P}}$, $\ddot{\mathbf{P}}$, or $\dddot{\mathbf{P}}$ represents the first, second or third derivative of $\mathbf{P}$ with respect to t. As described in [11, 5], curvature monotonicity can be verified by the numerator of $\frac{d\kappa}{ds}$, which can be represented as a Bernstein polynomial of degree $4n-7$ for 2D polynomial curves:

$$\lambda(t) = \sum_{i=0}^{4n-7} B_i^{4n-7}(t)\xi_i. \tag{2.3}$$

By utilizing the Bernstein form equation for the numerator of $\frac{d\kappa}{ds}$ as described in [5], a single fragment shader code can be used for Bézier curves of degree n. In the fragment shader, only degree-specific parts are dynamically replaced within the application program. If we opt not to use the equation from [5], we would need to generate code for Bézier curves of each degree by simplifying ξ_i, for example, using 'FullSimply' function in Mathemtica.

Theoretical curvature monotonicity region based on the sufficient condition:

For a Bézier curve, if $\lambda(t) \geq 0$ or $\lambda(t) \leq 0$ within $t \in [0\ 1]$, the curvature is monotonically varying. Note that ξ_is may have different signs even if the curvature is monotonically varying. As an example, Fig. 1 shows a cubic Bézier curve, its curvature plot and $\lambda(t)$. ξ_is are scaled so that they are $|\xi_i| \leq 1$. Although the signs of ξ_is are different, $\lambda(t) \geq 0$ for $t \in [0\ 1]$.

To simplify the situation, we investigate these regions based on the sufficient condition, which we refer to as the "*sufficient region*". The sufficient region is defined by $\xi_i \leq 0$ for curves with monotonically decreasing curvature or $\xi_i \geq 0$ for curves with monotonically decreasing curvature, where $0 \leq i \leq 4n-7$. Concerning the sufficient region of a control point $\mathbf{P}_j$ $(0 \leq j \leq n)$, it is the intersection of all $\xi_i \geq 0$ (or $\xi_i \leq 0$) with $\mathbf{P}_j$ representing a variable associated with ξ_i. Note that the region may have multiple areas.

The visualization of ξ_i is performed by using a GPU. To visualize the region of ξ_i for $\mathbf{P}_j$, we compute the value of ξ_i in the fragment shader by replacing the coordinate of $\mathbf{P}_j$ with the coordinates corresponding to each pixel in a window. When we visualize ξ_i for decreasing curvature, the corresponding pixel is painted with a user-specified color if $\xi_i < 0$. Otherwise, the pixel remains white. When we visualize ξ_i for increasing curvature, the corresponding pixel is painted if $\xi_i > 0$. By repeating the computation of ξ_i by $4n-7$ times and appropriately synthesizing the colors, we can simultaneously visualize all ξ_is. To show the boundary of ξ_i using anti-aliasing as in Fig. 2, the values of ξ_i at surrounding 8 pixels are also computed.

As an example, we demonstrate a 2D polynomial cubic Bézier curve with $\mathbf{P}_0 = [0\ 0]^{\mathrm{T}}$, $\mathbf{P}_1 = [1\ 0]^{\mathrm{T}}$, $\mathbf{P}_2 = [3\ 1]^{\mathrm{T}}$, $\mathbf{P}_3 = [4\ 5]^{\mathrm{T}}$. Fig. 2 illustrates the curvature monotonicity region for each control point, along with the control polygon and the curve. In the theoretical regions, regions with $\xi_i \geq 0$ are colored while the regions $\xi_i < 0$ remain white. Therefore, the theoretical sufficient regions are colored with white. For each control point $\mathbf{P}_j$, $\xi_i = 0$ is an implicit curve of x_j and y_j. The sufficient regions and the exact region where $\lambda(t) \leq 0$ or $\lambda(t) \geq 0$ are computed using the method proposed in [11]. Note that the theoretical sufficient regions are identical to the sufficient regions. Fig. 3 shows each ξ_i for $\mathbf{P}_j$.

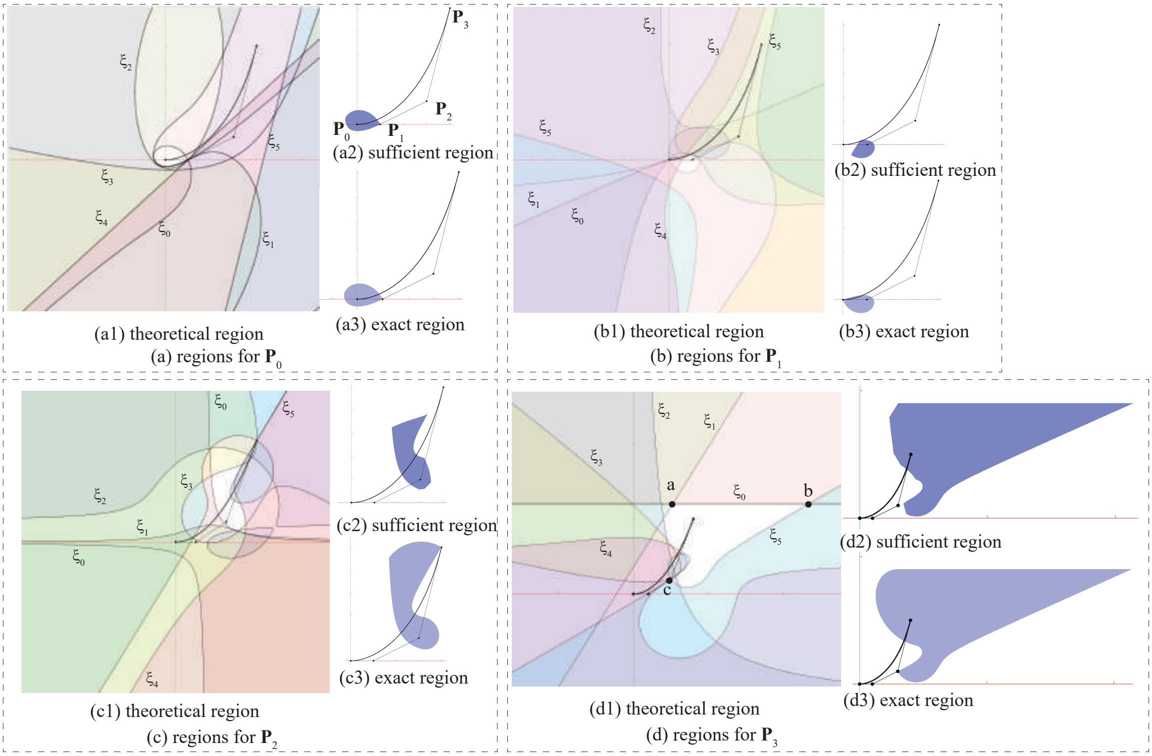

Fig. 2: Curvature monotonicity regions for each control point.

In the theoretical region of $\mathbf{P}_0$ in Fig. 2(a1), $\xi_0 = 0$ and $\xi_1 = 0$ represent implicit cubic curves. $\xi_2 = 0$ and $\xi_3 = 0$ are implicit quadratic curves. In this case, $\xi_2 = 0$ forms an ellipse and $\xi_3 = 0$ represents a hyperbola. $\xi_4 = 0$ and $\xi_5 = 0$ are both lines. $\xi_0 = 0$, $\xi_1 = 0$, and $\xi_2 = 0$ intersect at $\mathbf{P}_1$. Note that $\xi_4 = 0$ intersects with $\mathbf{P}_1$ in this specific case, but not necessarily in a general context. Upon careful examination of the theoretical region, it becomes evident the boundary is defined by $\xi_0 = 0$ and $\xi_1 = 0$.

In the theoretical region of $\mathbf{P}_1$ in Fig. 2(b1), $\xi_i = 0$ $(0 \leq i \leq 4)$ represent implicit cubic curves. $\xi_5 = 0$ is an implicit quadratic curve, which takes the form of a hyperbola in this context. $\xi_0 = 0$, $\xi_1 = 0$ and $\xi_2 = 0$ intersect at $\mathbf{P}_0$. The boundary of the theoretical region is defined by $\xi_0 = 0$ and $\xi_4 = 0$.

In the theoretical region of $\mathbf{P}_2$ in Fig. 2(c1), $\xi_0 = 0$ represents an implicit quadratic curve, which takes the form of a hyperbola in this context. ξ_i $(1 \leq i \leq 5)$ represent implicit cubic curves. ξ_3, ξ_4 and ξ_5 intersect at $\mathbf{P}_3$. The boundary of the theoretical region is defined by $\xi_0 = 0$, $\xi_2 = 0$,$\xi_3 = 0$, $\xi_4 = 0$ and $\xi_5 = 0$. In the theoretical region of $\mathbf{P}_3$ in Fig. 2(d1), $\xi_0 = 0$ and $\xi_1 = 0$ are lines. $\xi_2 = 0$ and $\xi_3 = 0$

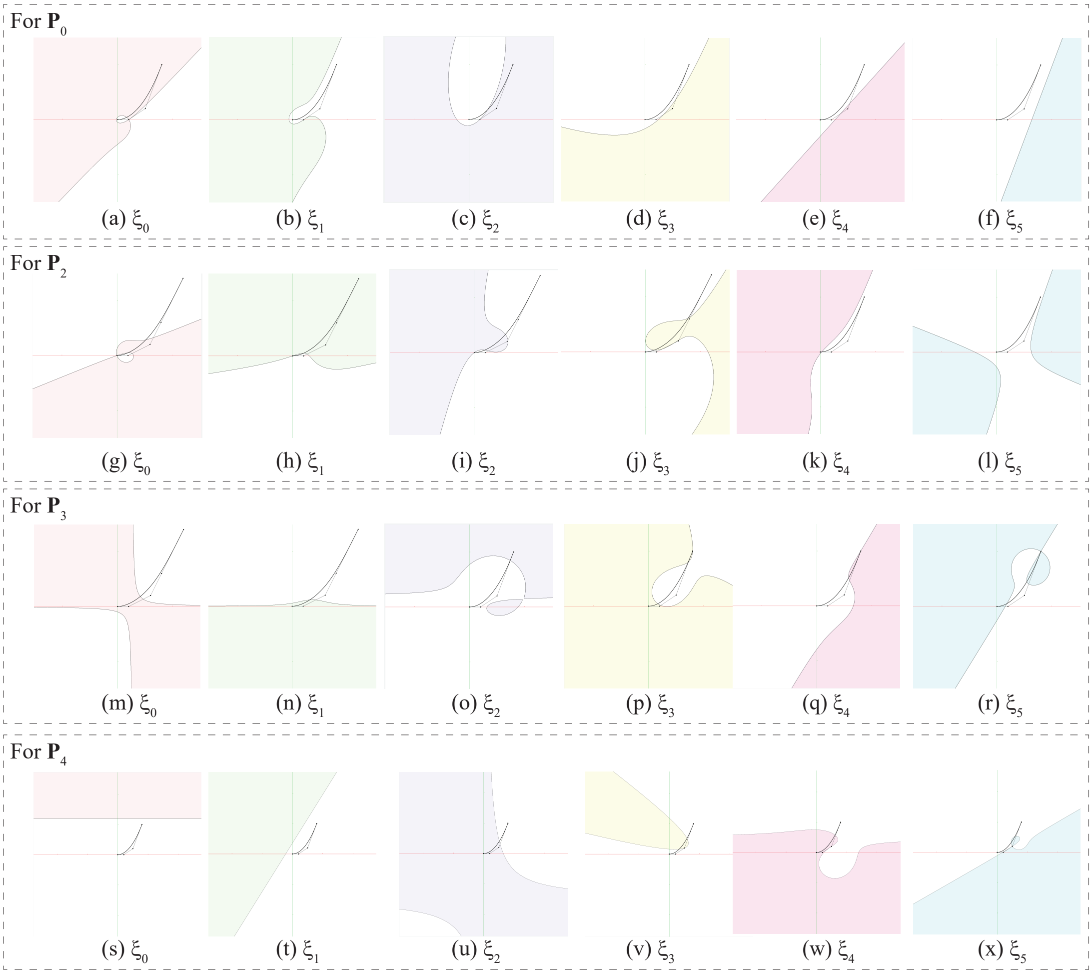

Fig. 3: ξ_is for $\mathbf{P}_0$, $\mathbf{P}_1$, $\mathbf{P}_2$, and $\mathbf{P}_3$.

are quadratic implicit curves, taking the form of hyperbolas in this case. $\xi_4 = 0$ and $\xi_5 = 0$ are implicit cubic curves. $\xi_3 = 0$, $\xi_4 = 0$ and $\xi_5 = 0$ go through P_2. The boundary of the theoretical region is defined by all ξ_is.

Table 1 shows the general characteristics of ξ_is of 2D cubic Bézier curves. For example, ξ_0 is an implicit cubic with respect to x_0 (or y_0) and goes through $\mathbf{P}_1$. These characteristics are verified using Mathematica and do not depend on the position of control points, except in degenerate cases.

If $\xi_0 = 0$ or $\xi_5 = 0$ serves as a boundary for the theoretical region, it also forms the boundary of the exact region. In Fig. 2(a1), $\xi_0 = 0$ occupies most of the boundary of the exact region. In Fig. 2(d1), $\xi_0 = 0$ from point a to point b, and $\xi_5 = 0$ from point b to point c, coincide with the boundary of the exact region.

In our analysis, we examined theoretical curvature monotonicity regions based on the sufficient conditions. This allows us to provide a partial explanation for the curvature monotonicity regions, especially when the sizes between the exact regions and the sufficient regions are similar, as depicted in Fig. 2.

Table 1: Characteristics of ξ_i of 2D cubic Bézier curves.

	$\mathbf{P}_0$						$\mathbf{P}_1$					
	ξ_0	ξ_1	ξ_2	ξ_3	ξ_4	ξ_5	ξ_0	ξ_1	ξ_2	ξ_3	ξ_4	ξ_5
degree	3	3	2	2	1	1	3	3	3	3	3	2
goes thrh	$\mathbf{P}_1$	$\mathbf{P}_1$	$\mathbf{P}_1$	-	-	-	$\mathbf{P}_0$	$\mathbf{P}_0$	$\mathbf{P}_0$	-	-	-
	$\mathbf{P}_2$						$\mathbf{P}_3$					
	ξ_0	ξ_1	ξ_2	ξ_3	ξ_4	ξ_5	ξ_0	ξ_1	ξ_2	ξ_3	ξ_4	ξ_5
degree	2	3	3	3	3	3	1	1	2	2	3	3
goes thrh	-	-	-	$\mathbf{P}_3$	$\mathbf{P}_3$	$\mathbf{P}_3$	-	-	-	$\mathbf{P}_2$	$\mathbf{P}_2$	$\mathbf{P}_2$

Conclusions:

We analyzed the curvature monotonicity regions of 2D polynomial Bézier curves based on the sufficient condition. Although we showed theoretical sufficient regions of a cubic Bézier curve, our program can handle higher degree curves. With the use of a GPU, we can interactively move a control point and can show the sufficient region with all implicit curves (ξ_is) in real time. We are currently extending the idea to rational curves and 3D curves.

Norimasa Yoshida, https://orcid.org/000-0000-1234-5678
Takafumi Saito, https://orcid.org/0000-0001-5831-596X

References:

[1] Farin, G.: Class A Bézier curves, Computer Aided Geometric Design, 23(7), 2006, 573-581, http://dx.doi.org/10.1016/j.cagd.2006.03.004

[2] Frey, W. H.; Field, D.A.: Designing Bézier conic segments with monotone curvature. Computer Aided Geometric Design, 17(6), 457-483, 2000. http://dx.doi.org/10.1016/S0167-8396(00)00011-X

[3] Mineur, Y.; Lichah T.; Castelain, J.M.; Giaume, H.: A shape controlled fitting method for Bézier curves. Computer Aided Geom Design 15(9), 1998, 879-891. http://dx.doi.org/10.1016/S0167-8396(98)00025-9

[4] Romani, L.; Viscardi, A.: Planar class A Bézier curves: The case of real eigenvalues. Computer Aided Geometric Design, 89, 2021. http://doi.org/10.1016/j.cagd.2021.102021

[5] Saito, T.; Yoshida, N.: Curvature monotonicity evaluation functions on rational Bézier curves, Computers & Graphics, 114,2023, 219-229. https://doi.org/10.1016/j.cag.2023.05.019

[6] Sánchez-Reys J.: Algebraic manipulation in the Bernstein form made simple via convolutions. Computer Aided Design, 35(10), 2003, 959-967. http://dx.doi.org/10.1016/S0010-4485(03)00021-6

[7] Sapidis, N. S.; Frey, W. H.: Controlling the curvature of a quadratic Bézier curve, Computer Aided Geometric Design, 9, 1992, 85-91. https://doi.org/10.1016/0167-8396(92)90008-D

[8] Tong, W.; Chen, M.: A sufficient condition for 3D typical curves. Computer Aided Geometric Design, 87, 2021. http://doi.org/10.1016/j.cagd.2021.101991

[9] Wang, A.; He. C.; Zheng, J.; Zhao, G.: 3D Class A Bézier curves with monotone curvature, Computer-Aided Design, 159, 2023.

[10] Walton, D. J.; Meek, D. S.: A Pythagorean hodograph quintic spiral, Computer Aided Design, 28(12), 1996, 943-950. http://dx.doi.org/10.1016/0010-4485(96)00030-9

[11] Yoshida, N.; Sakurai, S.; Yasuda, H.; Inoue, T.; Saito, T.: Visualization of the Curvature Monotonicity Regions of Polynomial Curves and its Application to Curve Design, Computer-Aided Design and Applications, 21(1), 2024, 75-87. https://doi.org/10.14733/cadaps.2024.75-87